TITLE
ASP Conference Series, Vol. **VOLUME**, **PUBLICATION YEAR**
EDITORS

Atomic Processes in Planetary Nebulae

Sultana N. Nahar
Department of Astronomy, The Ohio State University, Columbus, OH 43210, USA

Abstract. A hot central star illuminating the surrounding ionized H II region usually produces very rich atomic spectra resulting from basic atomic processes: photoionization, electron-ion recombination, bound-bound radiative transitions, and collisional excitation of ions. Precise diagnostics of nebular spectra depend on accurate atomic parameters for these processes. Latest developments in theoretical computations are described, especially under two international collaborations known as the Opacity Project (OP) and the Iron Project (IP), that have yielded accurate and large-scale data for photoionization cross sections, transition probabilities, and collision strengths for electron impact excitation of most astrophysically abundant ions. As an extension of the two projects, a self-consistent and unified theoretical treatment of photoionization and electron-ion recombination has been developed where both the radiative and the dielectronic recombination processes are considered in an unified manner. Results from the Ohio State atomic-astrophysics group, and from the OP and IP collaborations, are presented. A description of the electronic web-interactive database, TIPTOPBASE, with the OP and the IP data, and a compilation of recommended data for effective collision strengths, is given.

1. Introduction

A planetary nebula may be thought of as an 'astrophysical laboratory' of atomic emission-line spectra. The spectra enable determination of its temperature, density, and abundances of elements. The precise spectral analyis require accurate atomic parameters for the radiative are collisional processes in the nebular plasma. The four basic atomic processes that dominant the nebular plasma are:
i) Radiative bound-bound transition for excitation or de-excitation:

$$X^{+Z} + h\nu \rightleftharpoons X^{+Z*},$$

where the ion, X, is of charge, Z.
ii) Photoionization (PI) by absorption of a photon:

$$X^{+Z} + h\nu \rightleftharpoons X^{+Z+1} + \epsilon,$$

The inverse process is the electron-ion radiative recombination (RR).
iii) Autoionization (AI) and dielectronic recombination (DR):

$$e + X^{+Z} \rightarrow (X^{+Z-1})^{**} \rightarrow \begin{cases} e + X^{+Z} & \text{AI} \\ X^{+Z-1} + h\nu & \text{DR} \end{cases}$$

where the intermediate doubly excited state, autoionizing state, introduces resonances in the atomic processes. The inverse process of DR is photoionization via the autoionizing state.
iv) The collisional process of electron-impact excitation (EIE)

$$e + X^{+Z} \rightarrow e' + X^{+Z*}*$$

is one of the primary processes for spectral formation in astrophysical plasmas.

Each process needs to be treated separately to obtain the relevant atomic parameters. Sample results for each process, obtained mainly under the OP (1995, 1996) and the IP (1993) for accurate atomic data and stellar opacities will be presented later. Astrophysical model applications, such as for plasma opacities, need a huge amount of atomic data as these deal with a large number of atomic levels over wide energy ranges. Consistent sets of atomic parameters can be obtained if the atom or the ion is described by the same wavefunction expansion in each process. This also reduces the uncertainty in applications involving different processes and approximations. The Close Coupling (CC) R-matrix mehtodology employed by the OP and IP enable the computation of such self-consistent sets of atomic parameters.

The large amount of atomic data and opacities obtained under the OP and the IP are available electronically through the existing database, TOPbase (Cunto et al. 1993), and through its planned extension TIPTOPBASE (C. Mendoza and the OP/IP team).

2. Theory

All calculations for the various atomic parameters of the dominant atomic processes are carried out using the accurate and powerful R-matrix method in the close-coupling approximation (e.g. Burke & Robb 1975, Seaton 1987, Berrington et al. 1987, Berrington et al. 1995). The total wavefunction for a (N+1) electron system in the CC approximation is described as:

$$\Psi_E(e + ion) = A \sum_i^N \chi_i(ion)\theta_i + \sum_j c_j \Phi_j(e + ion), \qquad (1)$$

where χ_i is the target ion or core wavefunction in a specific state $S_i L_i \pi_i$ or level $J_i \pi_i$, θ_i is the wavefunction of the interacting (N+1)th electron in a channel labeled as $S_i L_i (J_i) \pi_i \; k_i^2 \ell_i (SL\pi \; or \;\; J\pi)$; k_i^2 is the incident kinetic energy. Φ_j is the correlation functions of (e+ion) system that compensates the orthogonality condition and short range correlation interations. The complex resonant structures in photoionization, recombination, and in electron impact excitation are included through channel couplings.

Relativistic effects are included through Breit-Pauli approximation in intermediate coupling. The (N+1)-electron Hamiltonian in the Breit-Pauli approxi-

mation, as adopted in the Iron Project, is

$$H_{N+1}^{\rm BP} = H_{N+1}^{NR} + H_{N+1}^{\rm mass} + H_{N+1}^{\rm Dar} + H_{N+1}^{\rm so}, \tag{2}$$

where non-relativisitc Hamiltonian is

$$H_{N+1}^{NR} = \sum_{i=1}^{N+1} \left\{ -\nabla_i^2 - \frac{2Z}{r_i} + \sum_{j>i}^{N+1} \frac{2}{r_{ij}} \right\}. \tag{3}$$

$H_{N+1}^{\rm mass}$ is the mass correction term, $H_{N+1}^{\rm Dar}$ is the Darwin term, $H_{N+1}^{\rm so}$ is the spin-orbit interaction term. Spin-orbit interaction splits the LS terms into fine-structure levels labeled by $J\pi$ where J is the total angular momentum. Solutions of the Schrodinger equation, $H_{N+1}^{BP}\Psi = E\Psi$ which becomes a set of coupled equations with the CC expansion, give the bound wavefunctions, Ψ_B, for negative energies, E < 0, and continuun wavefunction, Ψ_F, for positive energies, E ≥ 0.

The transition matrix elements for various atomic processes are:
$< \Psi_B||\mathbf{D}||\Psi_F >$ for photoionization and recombination,
$< \Psi_B||\mathbf{D}||\Psi_{B'} >$ for oscillator strength,
$< \Psi_F|H(e+ion)|\Psi_{F'} >$ for electron impact excitation,
where $\mathbf{D}$ is the dipole operator.

The transition matrix element with the dipole operator can be reduced to the generalized line strength defined, in either length or velocity form, as

$$S_{\rm L} = \left| \left\langle \Psi_f | \sum_{j=1}^{N+1} r_j | \Psi_i \right\rangle \right|^2, \quad S_{\rm V} = \omega^{-2} \left| \left\langle \Psi_f | \sum_{j=1}^{N+1} \frac{\partial}{\partial r_j} | \Psi_i \right\rangle \right|^2. \tag{4}$$

where ω is the incident photon energy in Rydberg units, and Ψ_i and Ψ_f are the wave functions representing the initial and final states, respectively.

The oscillator strength f_{ij} and the transition probability A_{ji} for the bound-bound transition can be obtained from S as

$$f_{ij} = \frac{E_{ji}}{3g_i} S, \quad A_{ji}(a.u.) = \frac{1}{2}\alpha^3 \frac{g_i}{g_j} E_{ji}^2 f_{ij}, \tag{5}$$

where E_{ji} is the transition energy, α is the fine structure constant, and g_i, g_j are the statistical weight factors of the initial and final states. The lifetime, τ_j, of a level j can be obtained from the transition probabilities decaying to the lower levels as $\tau_j = (\sum_i A_{ji}(s^{-1}))^{-1}$, where $A_{ji}(s^{-1}) = \frac{A_{ji}(a.u.)}{\tau_0}$ and $\tau_0 = 2.4191 \times 10^{-17}$s.

The photoionization cross section (σ_{PI}) is proportional to the generalized line strength (S),

$$\sigma_{PI} = \frac{4\pi}{3c} \frac{1}{g_i} \omega S. \tag{6}$$

The calculations of total electron-ion recombination employs a new unified treatment (Nahar & Pradhan 1994,1995). The method considers the infinite number of recombining states and incorporates the radiative and dielectronic recombinations, RR and DR, in a unified manner. The contributions to recombination from states with $n \leq 10$ are obtained from σ_{PI} using principle of

detailed balance, while the resonant contributions from states with $10 < n \leq \infty$ are obtained from an extension of the DR theory of Bell & Seaton (1985).

The recombination cross section, σ_{RC}, is related to σ_{PI} through the principle of detailed balance,

$$\sigma_{RC} = \sigma_{PI} \frac{g_i}{g_j} \frac{h^2\omega^2}{4\pi^2 m^2 c^2 v^2}. \tag{7}$$

The recombination rate coefficient, α_{RC}, is obtained as

$$\alpha_{RC}(T) = \int_0^\infty v f(v) \sigma_{RC} dv, \tag{8}$$

where $f(v)$ is the Maxwellian velocity distribution function. The total α_{RC} is obtained from contributions from infinite number of recombined states.

The collision strength for transition by electron impact excitation from the initial state of the target ion S_iL_i to the final state S_jL_j is given by

$$\Omega(S_iL_i - S_jL_j) = \frac{1}{2} \sum_{SL\pi} \sum_{l_i l_j} (2S+1)(2L+1) |\mathbf{S}^{SL\pi}(S_iL_il_i - S_jL_jl_j)|^2, \tag{9}$$

where $\mathbf{S}$ is the scattering matrix. The effective collision strength or the Maxwellian averaged collision strength can be obtained as

$$\Upsilon(T) = \int_0^\infty \Omega_{ij}(\epsilon_j) e^{\frac{-\epsilon_j}{kT}} d(\epsilon_j/kT). \tag{10}$$

which give the excitation rate coefficient, $q_{ij}(T) = (8.63\times10^{-6}/\omega_i T^{1/2}) e^{-E_{ij}/kT} \Upsilon(T)$ in $cm^3 s^{-1}$. where T is in K, $E_{ij} = E_j - E_i$, $E_i < E_j$ are in Rydbergs (1/kT = 157885/T), and j is the excited upper state.

3. Results and Discussions

Sample results for each atomic process are presented, e.g., for f-values, σ_{PI}, $\alpha_R(T)$, and $\Upsilon(T)$, in the following subsections.

3.1. Bound-Bound transitions

Due to fine structure, extensive sets of data for f- and A-values can be obtained for a large number of bound-bound transitions using the Breit-Pauli R-matrix method. In contrast to dipole allowed LS multiplets, BPRM method includes relativistic effects, and consideration of both the dipole allowed and intercombination transitions. The fine structure energy levels are analysed with quantum defects to obtain the spectroscopic identification, $(C_t\ S_t\ L_t\ J_t\ \pi_t n\ell)SLJ\ \pi$ where $(C_t\ S_t\ L_t\ J_t\ \pi_t)$ denotes the core configuration, spin, orbital, total angular momenta and parity, nl is configuration of the outer or valence electron, SL are the possible spin and orbital angular momenta, and $J\pi$ are the total angular momentum and parity of the (N+1)-electron system. The fobidden quadrupole (E2) and magnetic dipole (M1) transitions are treated with atomic structure calculations using codes such as SUPERSTUCTURE (Eissner et al. 1974).

Accurate fine structure transition probabilities have been obtained for a number of ions such as:
Li-like: C IV, N V, O VI, F VII, Ne VIII, Na IX, Mg X, Al XI, Si XII, S XIV, Ar XVI, Ca XVIII, Ti XX, Cr XXII, Ni XXVI
Fe ions: Fe V, Fe XVII, Fe XXI, Fe XXIII, Fe XXIV, Fe XXV
Other ions: C II, C III, O IV, S II, Ar XIII

The first large-scale application of the BPRM method for a complex ion, Fe V, resulted in 3865 fine structure energy levels, compared to 179 observed, and about 1.46 million f- and $A-$values for dipole allowed and intercombination (E1) transitions and 362 forbidden (E2,M1) transitions (Nahar et al. 2000). Table I presents a sample with complete spectroscopic identification of the transition array $3d^4(^4D) - 3d^3(^4F)4p(^5F^o)$ in Fe V.

Table I: Transition probabilities of Fe V. g=2J+1.

$level_i$	$level_j$	g_i	g_j	$E_i(Ry)$	$E_j(Ry)$	f	$A(sec^{-1})$
$3d^4(^5D)$	$3d^3(^4F)4p(^5F^o)$	1	3	5.5132	3.1644	2.154E-01	3.18E+09
$3d^4(^5D)$	$3d^3(^4F)4p(^5F^o)$	3	3	5.5119	3.1644	3.790E-04	1.68E+07
$3d^4(^5D)$	$3d^3(^4F)4p(^5F^o)$	3	5	5.5119	3.1496	1.358E-03	3.65E+07
$3d^4(^5D)$	$3d^3(^4F)4p(^5F^o)$	5	3	5.5094	3.1644	4.617E-02	3.40E+09
$3d^4(^5D)$	$3d^3(^4F)4p(^5F^o)$	5	5	5.5094	3.1496	5.967E-02	2.67E+09
$3d^4(^5D)$	$3d^3(^4F)4p(^5F^o)$	5	7	5.5094	3.1443	1.462E-02	4.69E+08
$3d^4(^5D)$	$3d^3(^4F)4p(^5F^o)$	7	5	5.5058	3.1496	6.895E-03	4.30E+08
$3d^4(^5D)$	$3d^3(^4F)4p(^5F^o)$	7	7	5.5058	3.1443	5.889E-02	2.64E+09
$3d^4(^5D)$	$3d^3(^4F)4p(^5F^o)$	9	7	5.5015	3.1443	1.966E-03	1.13E+08
$3d^4(^5D)$	$3d^3(^4F)4p(^5F^o)$	7	9	5.5058	3.1391	3.262E-02	1.14E+09
$3d^4(^5D)$	$3d^3(^4F)4p(^5F^o)$	9	9	5.5015	3.1391	5.139E-02	2.30E+09
$3d^4(^5D)$	$3d^3(^4F)4p(^5F^o)$	9	11	5.5015	3.1343	7.548E-02	2.78E+09
$3d^4(^5D)$	$3d^3(^4F)4p(^5F^o)$	25	35	5.5055	3.1451	1.068E-01	3.42E+09

3.2. Photoionization and Recombination

The photoionization cross sections, σ_{PI}, are calculated including autoionizing resonances that can enhance the background cross sections considerably. Fig. 1 shows the photoionization cross sections of the gound states of Fe I to Fe V (Bautista & Pradhan 1998). Extensive resonances dominate the cross sections for these complex ions. The enhancement in the backgound is up to three orders of magnitude for Fe I, over an order or magnitude for Fe II, and $\sim 50\%$ for Fe III.

For simpler systems the accuracy of theoretical cross sections can be tested against experimental data. Very precise measurements of σ_{PI} are now being carried out at a few places, such as the Advanced Light Source at Berkeley (e.g. Covington et al. 2001), the merged photon-ion beam set-up at Aahus University (Kjeldsen et al. 1999), and a synchroton based experiment at University of Paris-Sud (Wuilleumier et al., private communication). An example of the comparison of ground state photoionization cross sections of C II, with very good agreement

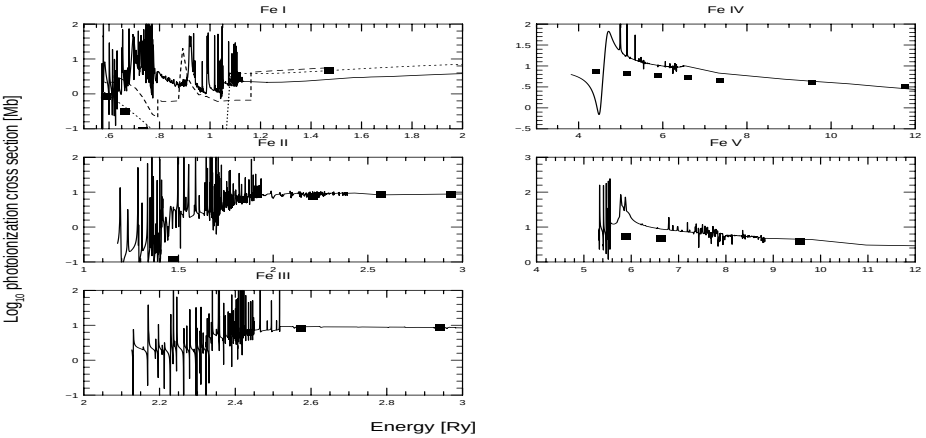

Figure 1. Photoionization cross sections, σ_{PI}, of the ground states of Fe I - Fe V.

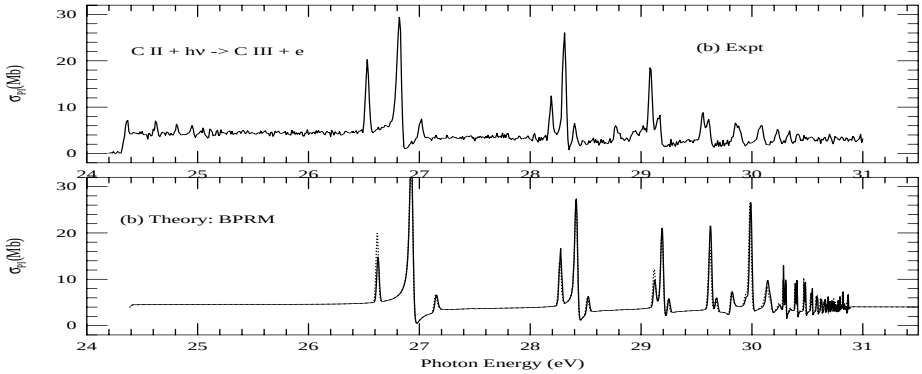

Figure 2. Comparison of theoretical and experimental photoionization cross sections, σ_{PI}, of the ground state fine structure levels $2s^2 2p(^2P^o_{1/2,3/2})$ of C II (Nahar 2002).

with experiment, is shown in Fig. 2. Theoretical calculations include relativistic fine structure.

An example of the total unified recombination rate coefficient $\alpha_R(T)$ for O III is presented in Fig. 3 (solid) (Nahar 1998). The earlier results are RR rates (dashed, Pequignot et al. 1991), low temperature DR rates (dotted, Nussbaumer & Storey 1983), high temperature DR rates by Badnell & Pindzolla (1990, short-dash-long-dash) and by Shull & Steenberg (1982, dot-desh). Differences can be noticed between the present unified values and the sum of the earlier (RR+DR) results, especially in the low and intermediate temperature. Compared to the earlier Shull & Steenberg results, autoionization into excited levels in the high temperature region reduces the recombination rates significantly.

The unified treatment for the total recombination provides rates that are valid over a wide range of temperatures for all practical purposes in contrast to addition of RR and DR rates obtained using different approximations for dif-

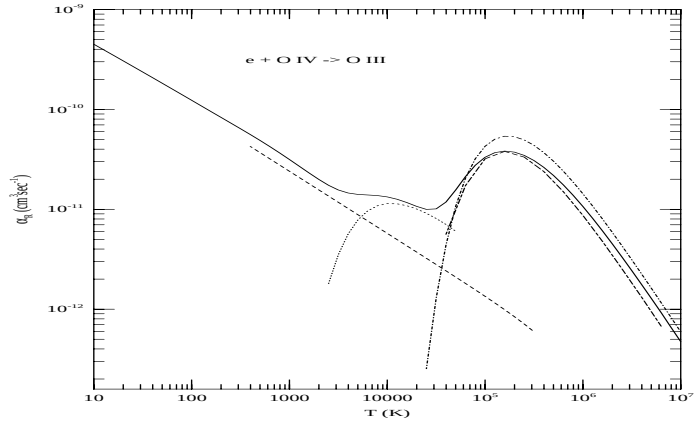

Figure 3. Comparison of the unified total recombination rate coefficients ($\alpha_R(T)$ (solid) with the previous calculations.

ferent temperature ranges. The method enables obtaining self-consistent sets of photoionization and recombination cross sections by using the identical wavefunction expansion for both the inverse processes. Following is the list of atoms and ions for which self-consistent sets of σ_{PI} and $\alpha_R(T)$ have so far been obtained for over 45 ions (e.g. Nahar & Pradhan 1997, *http* : *//www.astronomy.ohio* − *state.edu/* ∼*pradhan*):
Carbon: C I, C II, C III, C IV, C V, C VI
Nitrogen: N I, N II, N II, N IV, N V, N VI, N VI
Oxygen: O I, O II, O III, O IV, O V, O VI, O VII, O VII
Iron: Fe I, Fe II, Fe III, Fe IV, Fe V, Fe XIII, Fe XVII, Fe XXI, Fe XXIV, Fe XXV, Fe XXVI
C-like: F IV, Ne V, Na VI, Mg VII, Al VIII, Si IX, S XI, Ar XIII, Ca XV
Other ions: Si I, Si II, S II, S III, Ar V, Ca VII, Ni II
The data include the state specific recombination rates for hundreds of bound levels with n$\leq$ 10 for each ion.

The self-consistent sets of photoionization/recombination data include new photoionization cross sections that are generally an improvement over the OP data since more extensive and accurate eigenfunction expansions are employed.

3.3. Electron Impact Excitation

Reviews and compilations of available theoretical data sources are: *An evaluated compilation of theoretical data sources for electron-impact excitation of atomic ions*, (A.K. Pradhan & J.W. Gallagher, Atomic Data and Nuclear Data Tables, 52, 227, 1992), and *Electron Collisions with Atomic Ions* (A.K. Pradhan & H.L. Zhang, in LANDÖLT-BORNSTEIN Volume *Atomic Collisions*, Ed. Y. Itikawa, Springer-Verlag, in press).

A table of recommended data for effective collision strengths and A-values for nebular ions is available on-line from www.astronomy.ohio-state.edu/∼pradhan

The aim of the IP is to compute collisional data for the iron-peak elements in various ionization stages. Of the 50 publications in the "Atomic data from the IRON Project" series in Astronomy and Astrophysics journal, most are on

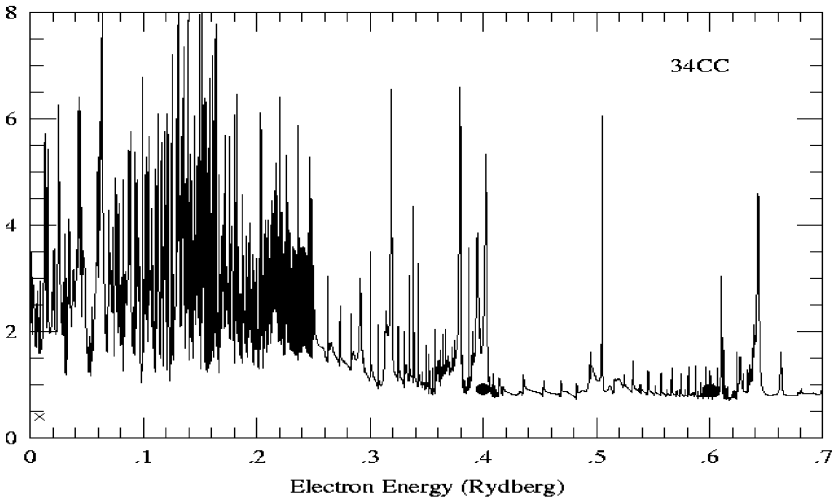

Figure 4. Collision strength for the first transition in Fe VI $\Omega(^4F_{3/2} - {}^4F_{5/2})$ from the Iron Project CC R-matrix calculation (Chen & Pradhan 1999); previous results (• - Nussbaumer & Storey 1978, × - Garstang et al. 1978) neglect resonances.

collisional strengths. At present the Iron Project website is maintained by Keith Butler at: *www.usm.uni − muenchen.de/people/ip/iron − project.html*

An example of IP calculations for iron ions is the recent work on Fe VI (Chen & Pradhan 1999). Fig. 4 presents the detailed collision strength $\Omega(E)$ showing extensive resonance structure. Previous calculations neglecting resonances seriously underestimate the Maxwellian averaged effective collision strength $\Upsilon(T)$ (Eq. 10) by several factors.

4. TIPTOPBASE: atomic radiative and collisional data

The existing electronic archive for the OP data, TOPbase (*http* : *//heasarc.gsfc.nasa.gov* at Goddard, NASA and *http* : *//vizier.u − strasbg.fr/OP.html* at CDS) contain (i) photoionization cross sections of bound LS terms for ~ 200 ions with Z = 1 - 14, 16, 18, 20, 26, (ii) energy levels and transition probabilities ($\sim 10^7$ f-values), (iii) monochromatic and Rosseland mean opacities (at CDS only)

The new database, TIPTOPbase (under development, C. Mendoza & the OP/IP team) will have radiative and collisional data from the OP and the IP. The data include:

(i) All data from TOPbase (and replacement of improved data), (ii) collisional data for iron and iron peak elements, (iii) new elements through all ionization stages: P, Cl, K, as well as selected ions such as Ni II and Ni III, (iv) updated sets of radiative data from new CC calculations, (v) "Tail" photoionization cross sections at high energies that include inner-shell ionization, (vi) total and level specific recombination rate coefficients, (vi) additional data for f-values including inner-shell excitations in iron ions Fe VIII - XIII ("PLUS" data) calculated with SUPERSTRUCTURE, (vii) radiative data (σ_{PI} and f-values) for fine structure levels including relativistic effects, (viii) on-line com-

putational facilities for opacities and radiative accelerations for user-specified mixtures of elements ("customized" opacities and radiative forces) (see IP in Extended Abstracts).

5. Conclusion

The current status of large-scale ab initio close coupling R-matrix calculations for radiative and collisional processes is reported. The Iron Project Breit Pauli R-matrix radiative calculations include large numbers of dipole allowed and inter-combination transitions. Self-consistent sets of atomic data for photoionization and unified (electron-ion) recombination (including RR and DR) are obtained, and should yield more accurate photoionization models. Work is in progress for heavy ions of the iron group elements.

Acknowledgments. This work is supported partially by the U.S. National Science Foundation and NASA.

References

Bautista, M.A. & Pradhan, A.K. 1998, ApJ, 492, 650

Berrington, K.A., Burke, P.G., Butler, K., Seaton, M.J., Storey, P.J., Taylor, K.T., & Yu, Yan, 1987, J.Phys. B, 20, 6379

Berrington, K.A., Eissner, W.B., & Norrington, P.H. 1995, CPC, 92, 290

Burke, P.G. & Robb, W.D. 1975, Adv. At. Mol. Phys., 11, 143

Chen, G.X. & Pradhan, A.K. 2000, ApJS, 147, 111

Covington et al. 2001, Phys.Rev.Lett. 87, 243002

Cunto, W., Mendoza, C., Ochsenbein, F., Zeippen, C.J, 1993, A&A, 275, L5

Eissner, W., Jone, S. W., & Nussbaumer, N. 1974, CPC, 8, 270

Hummer, D.G., Berrington, K.A., Eissner, W., Pradhan, A.K., Saraph, H.E., & Tully, J.A. 1993, A&A, 279, 298

Kjeldsen, H., Folkmann, F., Hensen, J.E., Knudsen, H., Rasmussen, M.S., West, J.B., & Andersen, T. 1999, ApJ. 524, L143

Nahar S.N. 1999, ApJS, 120, 131

Nahar S.N. 2002, Phys.Rev.A (in press)

Nahar S.N., Delahaye F.,Pradhan A.K., & Zieppen C.J. 2000, A&AS144, 141

Nahar, S.N. & Pradhan, A.K. 1994, Phys.Rev.A, 49, 1816; 1995, ApJ, 447, 966; Nahar, S.N 1996, Phys.Rev.A, 53, 1545

Nahar, S.N., & Pradhan, A.K. 1997, ApJS, 111, 339

Pequignot, D., Petitjean, P., & Boisson, C. 1991, A&A, 251, 680; Nussbaumer, H. & Storey, P.J. 1983, A&A, 126, 75; Badnell, N.R. & Pindzola, M.S. 1989, Phys.Rev.A, 39, 1690; Shull, J.M. & van Steenberg, M. 1982, ApJS, 48, 95

Seaton, M.J. 1987, J.Phys.B, 20, 6363

The Opacity Project 1 and 2, compiled by the Opacity Project team (Institute of Physices, London, UK, 1995, 1996)